

# Interplay between isoscalar and isovector correlations in neutron-rich nuclei

Ikuko Hamamoto<sup>1,2</sup> and Hiroyuki Sagawa<sup>1,3</sup>

<sup>1</sup> *Riken Nishina Center, Wako, Saitama 351-0198, Japan*

<sup>2</sup> *Division of Mathematical Physics,*

*Lund Institute of Technology at the University of Lund, Lund 22362, Sweden*

<sup>3</sup> *Center for Mathematics and Physics, University of Aizu,*

*Aizu-Wakamatsu, Fukushima 965-8580, Japan*

## Abstract

The interplay between isoscalar and isovector correlations in the  $1^-$  states in neutron-rich ( $N \neq Z$ ) even-even nuclei is studied, taking examples of the nuclei,  ${}^{22}_8\text{O}_{14}$  and  ${}^{24}_8\text{O}_{16}$ . The excitation modes explored are isovector dipole and isoscalar compression dipole modes. The self-consistent Hartree-Fock plus the random-phase approximation with the Skyrme interaction, SLy4, is solved in coordinate space so as to take properly into account the continuum effect. The isovector peak induced by isoscalar correlation, the isoscalar peak induced by isovector correlation, and the possible collective states made by both isoscalar and isovector correlations, ("iS-iV pigmy resonance"), are shown. The strong neutron-proton interaction in nuclei can be responsible for controlling the isospin structure of normal modes. It is explicitly shown that in the scattering by isoscalar (isovector) particles on  $N \neq Z$  even-even nuclei isovector (isoscalar) strength in addition to isoscalar (isovector) strength may be populated.

PACS numbers: 21.60.Jz, 21.10.Re, 21.10.Gv, 27.30.+t

## I. INTRODUCTION

The mutual interplay between isoscalar (IS) and isovector (IV) correlations in neutron-rich nuclei is explored in the present work. The interplay between IS and IV correlations and the related collective modes have been an attractive and centrally placed topic in the study of nuclear structure. The IV dipole giant resonance (GR) is the first established giant resonance which was found in the photo absorption reaction more than 50 years ago, while the corresponding IS partner is the center of mass motion which is identified as a spurious excitation mode. The IS quadrupole correlation is particularly strong in nuclei, and IS quadrupole GR is systematically found in experiments, while the corresponding IV partner is expected to lie in a higher energy with a broader width, but the systematics of the nature of the IV quadrupole GR is experimentally not yet well established. For example, see Ref. [1].

In the analysis of scattering data by IS particles such as  $\alpha$  particles it is often assumed that IS particles excite only IS strength. This assumption is generally incorrect if the target nuclei have  $N \neq Z$ . For example, in nuclei with neutron excess IS operators excite IS moments, however, the strong neutron-proton forces may tend to keep the local ratio of neutrons to protons. Then, the presence of neutron excess  $N > Z$  means that IV moments may be excited also by IS particles [2]. In Fig. 2 of Ref. [3] a numerical example of this phenomenon in  $^{48}\text{Ca}$  is shown. Namely, if only IS interaction is taken into account, no appreciable peak of IV strength is seen around the energy ( $\approx 16.5$  MeV) of IS quadrupole giant resonance (QGR). In contrast, a sharp IV peak appears at the energy of the IS QGR when IV interaction is further included in this nucleus with neutron excess.

The phenomena exchanging the above roles of IS and IV excitations in the response may be expected to be also true. Namely, IV operators may produce IS moments generally in nuclei with  $N \neq Z$  except for the case that the IS moment corresponds to the center of mass motion. To study this issue is one of the main points of the present work.

Isospin is not an exact but a pretty good quantum-number around the ground state of nuclei with both  $N=Z$  and  $|N-Z| \gg 1$ . In  $N=Z$  even-even nuclei IS and IV operators excite, roughly speaking, different states, since the isospin of the ground state,  $T_0$ , is in a good approximation equal to zero. In contrast, in  $N \neq Z$  even-even nuclei IS and IV operators can excite the same states, which have the same isospin  $T_0=(N-Z)/2$  as that of the ground

state. This situation is particularly interesting in nuclei with  $|N-Z|\gg 1$ , because the ratio of the population of excited states with  $T=T_0$  to that of higher-lying excited states with  $T=T_0+1$  by IV operator is the order of  $T_0$ . Namely, IV excitations to  $T=T_0$  states will consume the major part of the IV strength.

In the present work we choose to study the relation between the IV dipole (IVD) mode and the IS compression dipole (ISCD) mode. Both modes have spin-parity  $1^-$ , while various characters besides the isospin (for example, the r-dependence of the one-body operators or the difference between shape oscillation and compression) of the two modes are different. In stable nuclei the IVD GR appears energetically much lower than ISCD GR, the major part of which consists of  $3\hbar\omega$  excitations. In contrast, in neutron drip line nuclei a large fraction of ISCD strength is often expected to lie much lower than IVD GR [4]. In order to study the mutual influence by IS and IV modes, it is convenient to study the nuclei, in which considerable amounts of IVD and ISCD strengths may occur around the same energy region. Some such examples are the nuclei,  ${}^{22}_8\text{O}_{14}$  and  ${}^{24}_8\text{O}_{16}$ , both of which are expected to be spherical. This choice of nuclei was stimulated by Ref. [5] in which the measured photoneutron cross sections for  ${}^{22}\text{O}$  were reported though experimental error bars were large and by Ref. [6] in which the observation of the bound IS and IV dipole excitations in  ${}^{20}_8\text{O}_{12}$  was reported.

In Sec. II the model and the formalism used are briefly summarized, while in Sec. III numerical results of nuclei,  ${}^{22}\text{O}$  and  ${}^{24}\text{O}$ , are presented and we try to study especially the mutual influence between IS and IV correlations in the  $N>Z$  nuclei. In Sec. IV a summary and discussions are given.

## II. MODEL AND FORMALISM

We perform the self-consistent Hartree-Fock (HF) plus the random-phase approximation (RPA) with Skyrme interactions, including simultaneously both IS and IV interactions. The RPA response function is estimated in coordinate space so as to take properly into account the continuum effect. Choosing the Skyrme interaction SLy4 [7], the model and the formalism are the same as those employed in Ref. [4]. The choice of SLy4 is made because, among others, the calculated neutron separation energies of  ${}^{22}\text{O}$  and  ${}^{24}\text{O}$  are close to the measured ones and the calculated incompressibility in nuclear matter is a realistic value,

$K_0 = 229.9$  MeV.

Writing the one-body operators

$$D_\mu^{\lambda=1, \tau=1} = \sum_i \tau_z(i) r_i Y_{1\mu}(\hat{r}_i) \quad (1)$$

for IV dipole strength and

$$D_\mu^{\lambda=1, \tau=0} = \sum_i r_i^3 Y_{1\mu}(\hat{r}_i) \quad (2)$$

for IS compression dipole strength, we study the RPA strength function using the Green function

$$S(E) \equiv \sum_n \int |\langle n, E_n | D | 0 \rangle|^2 \delta(E - E_n) dE_n = \frac{1}{\pi} \text{Im Tr}(D^\dagger G_{RPA}(E) D) \quad (3)$$

where  $|n, E_n\rangle$  expresses an excited state with energy  $E_n$  including both discrete and continuum states. The transition density for an excited state  $|n\rangle$ ,

$$\rho_{n0}^{tr}(\vec{r}) \equiv \langle n | \sum_{i=1}^A \delta(\vec{r} - \vec{r}_i) | 0 \rangle \quad , \quad (4)$$

can be calculated from the RPA response, and the radial transition density  $\rho_n^{tr}(r)$  is defined by

$$\rho_{n0}^{tr}(\vec{r}) \equiv \rho_n^{tr}(r) Y_{\lambda\mu}(\hat{r}) \quad . \quad (5)$$

Now, in the case that the numerical calculations of the self-consistent HF+RPA could be performed with perfect accuracy, the spurious center-of-mass state would be degenerate with the ground state and there would be no spurious component in the excitation spectra. However, in numerical calculations it is, in practice, difficult to take away completely the dipole strength coming from the spurious component. A very small admixture of the spurious component can produce a pretty large strength especially in the ISCD response. Thus, we have to further eliminate the spurious component in the excitation spectra. Namely, as is often done, in the calculation of the IV dipole strength we use the operator

$$\bar{D}_\mu^{\lambda=1, \tau=1} = -\frac{2N}{A} \sum_i^{proton} r_i Y_{1\mu}(\hat{r}_i) + \frac{2Z}{A} \sum_i^{neutron} r_i Y_{1\mu}(\hat{r}_i) \quad , \quad (6)$$

instead of the operator (1). In the evaluation of the strength of IS compression dipole we use the operator

$$\bar{D}_\mu^{\lambda=1, \tau=0} = \sum_i^A (r_i^3 - \eta r_i) Y_{1\mu}(\hat{r}_i) \quad (7)$$

where  $\eta = \frac{5}{3} \langle r^2 \rangle$ , instead of the operator (2).

### III. NUMERICAL RESULTS

Oxygen isotopes are generally expected to be spherical, except for very neutron-deficient isotopes such as  ${}^8_8\text{O}_4$ , which is the mirror nucleus of  ${}^{12}\text{Be}$ . Here we study  ${}^{22}\text{O}$  and  ${}^{24}\text{O}$ , both of which are treated as spherical j-j shell closed nuclei.

First, we check whether in our present model we obtain the experimentally reported amount of ISCD strength in a bound state of  ${}^{16}_8\text{O}_8$ . From the analysis of  $(\alpha, \alpha')$  scattering it is reported that the  $1^-$  and  $T=0$  state at 7.12 MeV consumes about 4 percent of the ISCD energy-weighted sum-rule (EWSR) [8], while about twice the strength on the same state was reported from the analysis of the electron scattering data [9]. Applying our model to  ${}^{16}\text{O}$ , we obtain the ISCD strength of about 2 percent of ISCD EWSR as a sum of the strength of two bound RPA solutions at 10.4 and 10.8 MeV. Therefore, we expect that our calculation of ISCD spectrum can be reasonably realistic.

#### A. The nucleus ${}^{22}\text{O}$

Using the SLy4 interaction, we obtain the neutron and proton separation energies,  $S_n = 7.25$  MeV and  $S_p = 22.29$  MeV, compared with the experimental values,  $S_n = 6.85$  MeV and  $S_p = 23.26$  MeV.

In Fig. 1 we show the calculated RPA strength for ISCD operator. The solid curve is the strength when both IS and IV interactions are included in RPA, while the strength obtained by including only IS interaction in RPA is denoted by the dotted curve. No RPA solution is found below the threshold energy. We note the following points. (a) As was already found in Ref. [4] concerning the ISCD response in neutron drip line nuclei, we very often obtain a large portion of ISCD strength in the energy interval of several MeV above the threshold. This large strength appearing in the energy much lower than the energy of the ISCD GR, which is recognized as a very broad "resonance" found for  $E_x \gtrsim 24$  MeV in Fig. 1, comes from the possible presence of occupied weakly-bound low- $\ell$  neutron orbits together with the strong  $r$ -dependence ( $r^3$ ) of the ISCD operator. This point is later discussed in more detail in subsec. III. B related to Figs. 5 and 6 for  ${}^{24}\text{O}$ . (b) When IV interaction is included on the top of IS interaction, the heights of many lower-lying IS peaks become lower and the peak energies may shift to slightly higher energies via the IV components contained in those IS

peaks, due to the repulsive nature of the IV interaction. (c) There are some peaks denoted by the solid curve, which may not be understood in the way of the above (b). An example is the broad peak around 18.5 MeV in the solid curve. The nature of the IS peaks around 14.0 and 18.5 MeV, which have no trivial corresponding peaks in the dotted curve, is later discussed in comparison of Fig. 1 with Fig. 2.

In Fig. 2 the calculated RPA strength for IVD operator is shown as a function of excitation energy. The strength, in which both IS and IV interactions are included in RPA, is denoted by the solid curve, while the strength obtained by including only IV interaction in RPA is expressed by the long-dashed curve. No RPA solution is found below the threshold energy. The unperturbed particle-hole (p-h) strength, in which particle levels are in the continuum, is shown by the dotted curve, while the energies of seven unperturbed p-h excitations, in which particle levels are bound states, are shown by vertical arrows. There are two such neutron excitations and five such proton excitations. Since the contributions to the unperturbed strength by the excitations from such bound states to bound states have a dimension different from the dimension of the contributions by the excitations from bound states to continuum states due to the unavoidable difference between the normalization of bound states and that of continuum states, the two kinds of contributions cannot be shown in the same figure in a simple manner. So, we just show the p-h energies of the excitations from bound states to bound states. It is noted that the RPA result always contains the contributions by both excitations from bound to bound states and those from bound to continuum states.

It is known that in light nuclei such as oxygen isotopes even IVD GR does not appear as a clean large resonance, instead, it splits into several considerable peaks. Therefore, roughly speaking, the peaks in the region of  $E_x > 18$  MeV in Fig. 2 may be regarded as IVD GR of  $^{22}\text{O}$ . It is seen that the main peaks belonging to the IVD GR hardly change when IS interaction is included on the top of IV interaction. That means, those peaks hardly have IS components even in this nucleus with neutron excess. In contrast, several IV peaks between the threshold energy and about 16 MeV, which are obtained by including only IV interaction, seem to be reorganized to approximately one relatively broad peak with the peak energy around 14 MeV, when IS interaction is included. The reorganization is certainly made through the IS components contained in those several IV peaks.

In Fig. 3 the radial transition densities multiplied by  $r^2 r^3$  for IS and  $r^2 r$  for IV, which are

calculated at  $Ex = 18.5$  MeV in the continuum, are shown in arbitrary units, as a function of radial variable. Here the multiplied factor  $r^2$  expresses the volume element which appears in the integration over  $r$ . The total IV (= neutron – proton) transition density denoted by the thin solid curve shows, roughly speaking, a typical shape of the IVD GR transition density with a peak around the nuclear surface. An interesting feature found in Fig.3 is that the  $r$ -value of the (negative) inner peak (around 3.4 fm) of the total ISCD transition density is almost the same as that of the peak of the total IV transition density. This fact together with the creation of the relatively broad peak of ISCD strength when IV interaction is included on the top of IS interaction leads to the interpretation that the relatively broad ISCD peak around 18.5 MeV in Fig. 1 is induced by the IV peak at the same energy via the IV component contained in the ISCD peak.

In Fig. 4 the radial transition densities multiplied by  $r^2r^3$  for IS and  $r^2r$  for IV calculated at  $Ex = 14.0$  MeV in the continuum are shown in arbitrary units, as a function of radial variable. The total IV transition density has a peak around 4 fm clearly outside the nuclear surface, at which  $r$ -value the total IS (= neutron + proton) transition density expressed by the thick solid curve has approximately a node in contrast to the case of Fig. 3. Then, we may call the relatively broad peak around  $Ex = 14$  MeV, which appears in the solid curve expressing the final RPA result in both Fig. 1 and Fig. 2, pigmy resonance with both isoScalar and isoVector correlations ("iS-iV pigmy resonance"). The pigmy resonance is interpreted as neither the IS strength induced by a strong IV peak nor the IV strength induced by a strong IS peak, due to the presence of neutron excess. It is a relatively broad resonance, of which the energy is much lower than the energies of both IVD GR and ISCD GR, but it gathers the collectivity of low-lying IS and IV strengths. The IV dipole strength in the region of  $Ex = (11-16.5)$  MeV consumes 11.4 percent of the energy-weighted sum-rule (EWSR) and 16.6 percent of the non-energy-weighted sum-rule (NEWSR). For ISCD mode (see Fig. 1) we find even a larger portion of the contribution to the sum rule from the same energy region: 18.0 percent for EWSR and 25.9 percent for NEWSR. Such an iS-iV pigmy resonance will be found neither in stable nuclei because the peaks with appreciable strength of ISCD appear in the energy region different from that of IVD nor in  $N=Z$  nuclei because the isospin of ISCD states is 0 while that of IVD states is 1.

In the continuum RPA, we have no explicit values for the amplitudes of respective p-h components. Nevertheless, the collective nature of a given resonance can be seen from

the contribution to the sum rule and the number of available configurations. For IV  $1^-$  states in Fig. 2 we show the unperturbed response of the excitation to the continuum (by the dotted curve) and the p-h energies of the excitation to bound states (by arrows). In the energy region of  $E_x = 10-18$  MeV there are two resonance states and six bound p-h states. Starting from the lowest-energy peak, they are assigned as (a) neutron ( $2s_{1/2}, 1p_{1/2}^{-1}$ ), (b) neutron ( $1f_{7/2}, 1d_{5/2}^{-1}$ ) at 12.2 MeV with the width 1.22 MeV, (c) proton ( $2s_{1/2}, 1p_{1/2}^{-1}$ ), (d) proton ( $1d_{5/2}, 1p_{3/2}^{-1}$ ), (e) proton ( $1d_{3/2}, 1p_{1/2}^{-1}$ ), (f) neutron ( $1d_{3/2}, 1p_{1/2}^{-1}$ ) at 16.8 MeV with the width 83 keV, (g) neutron ( $2s_{1/2}, 1p_{3/2}^{-1}$ ), and (h) proton ( $2s_{1/2}, 1p_{3/2}^{-1}$ ). They get some finite width as shown by the long-dashed curve between 11 and 18 MeV due to the coupling to the continuum in RPA with IV interaction. The main configurations of respective peaks expressed by the long-dashed curve can be easily assigned to respective unperturbed peaks, because corresponding unperturbed peaks were pushed only slightly to higher energy due to the repulsive nature of IV interaction. Some strength of those low-lying unperturbed peaks must be shifted to the high-lying giant resonance due to the repulsive IV interaction. Nevertheless, the correspondence between the unperturbed and perturbed (only by IV interaction) peaks in the energy region of 11-17 MeV can be clearly seen in Fig. 2. When we further introduce IS interaction on the top of IV interaction, we obtain iS-iV pigmy resonance, of which the main component comes from the configurations above (in particular, five lower-energy configurations) and collect most of the strength around  $E_x=14$  MeV. As is seen in Fig.4, there are substantial contributions also from proton p-h excitations.

It is further noted that, for example, in Fig. 4 the  $r$ -values (about 3.3 fm and 9.2 fm), at which the curve of "neutron IS  $r^3$ " becomes zero, are clearly different from those, at which the curve of "neutron IV  $r$ " is zero. Since the multiplied factors  $r^3$  and  $r$  do not make such nodes, these nodes come from the nodes of the transition densities. Namely, the relevant calculated radial transition densities of "neutron IS  $r^3$ " and "neutron IV  $r$ " can be different in a subtle manner, though both neutron transition densities are calculated at the same energy. Solving the continuum RPA makes it possible to obtain the possible difference. If the RPA calculation were performed, for example, by expanding the wave functions in terms of a finite number of harmonic-oscillator bases, the difference would not have appeared, because the shapes (then, the nodes) of the radial transition densities for protons and neutrons at a given energy are uniquely determined since the bases have no intrinsic widths. In contrast, if two peaks, of which one is IS while the other is IV, with



finite widths occur energetically close to each other, the transition density at a given energy between the two peaks can be a mixture of the components of the two peaks. If so, the neutron (and proton) transition density for IS operator can be different from that for IV operator.

## B. The nucleus $^{24}\text{O}$

Using the SLy4 interaction, we obtain  $S_n = 4.88$  MeV and  $S_p = 24.62$  MeV, compared with the experimental values  $S_n = 4.19$  MeV and  $S_p = 27.11$  MeV.

By the solid curve in Fig. 5 we show the RPA strength, in which both IS and IV interactions are included in RPA, while the RPA strength with only IS interaction is shown by the dotted curve. No RPA solution is found below the threshold energy. The ISCD GR is recognized as a very broad bump with a peak at slightly above 30 MeV. As in the case of  $^{22}\text{O}$ , in the energy region much lower than ISCD GR we obtain many strong peaks. In particular, we note a huge calculated peak at 5.8 MeV with a width of a few MeV. The main component of the 5.8 MeV peak is the neutron (p-h) =  $(2p_{3/2}2s_{1/2}^{-1})$  configuration.

In Fig. 6 the radial transition density multiplied by  $r^2r$ , which corresponds to the center of mass motion, is plotted by the solid curve. The integration of the solid curve from  $r=0$  to infinity is zero if the 5.8 MeV  $1^-$  state contains no spurious component due to the center of mass motion. In other words, only after the integration over  $r$  the degree of the contamination of the spurious component can be seen. Radial transition densities of neutrons and protons are determined by the properties of excitation modes at given energies and are the same, for example, in the spurious strength (corresponding to the center of mass motion) and the ISCD strength. The difference between the contributions to the two kinds of strengths comes only from the different multiplication factors depending on  $r$ . It is noted that the solid curve in Fig. 6 extends considerably to the region far outside the size of the nucleus. If we multiply the solid curve further by  $r^2$  so as to obtain the ISCD strength, it is seen that the main contribution to the ISCD strength comes from the region far outside the nucleus. This peculiar situation comes from the characteristic behavior of the main component, the neutron (p-h) =  $(2p_{3/2}2s_{1/2}^{-1})$  configuration. The neutron  $2s_{1/2}$  level, which is the last occupied orbit, has an energy of  $-4.88$  MeV in the HF calculation, while the  $2p_{3/2}$  level is slightly before becoming a one-particle resonant level. Consequently, the

contribution to the radial transition density by the p-h configuration has an extended tail to the outside of the nucleus. Then, since the ISCD operator has the strong  $r$ -dependence ( $r^3$ ), this main component produces a very large ISCD strength making a large contribution to the ISCD sum-rule. Thus, it can be said that the strong peak at 5.8 MeV is not really the result of large collectivity but the peak is strong due to the unique behavior of the neutron low- $\ell$  wave functions.

In Fig. 7 the calculated RPA strength with the full interactions for the IVD operator is shown by the solid curve, while the RPA strength obtained by including only IV interaction in RPA is shown by the long-dashed curve. The unperturbed p-h strength for the IVD operator, in which particle states are in the continuum, is denoted by the dotted curve expressed as "unperturbed". The energies of the unperturbed p-h excitations, in which particle levels are bound states, are shown by vertical arrows. There are five such proton p-h excitations within the energy range of Fig. 7 and two such neutron p-h excitations. All unperturbed p-h excitations, in which particle states are in the continuum as well as bound states, contribute to the RPA solutions. The major component of the small bump in the solid curve, of which the peak is around 6.5 MeV, is the neutron (p-h) =  $(2p_{3/2}2s_{1/2}^{-1})$  configuration. Since the IVD operator has the mild  $r$ -dependence ( $r$ ), the response is not so strong as the ISCD response shown in Fig. 5, in spite of the fact that the IVD strength comes mainly from the outside of the nuclear surface.

The relation between the IV and IS correlations, which was obtained in subsec. III. A for  $^{22}\text{O}$ , is found also in  $^{24}\text{O}$  in a very similar manner. For example, the relatively sharp ISCD peak around 16.7 MeV in Fig. 5 can be interpreted as the one induced by the IVD peak at the same energy, as in the case of the 18.5 MeV ISCD peak of  $^{22}\text{O}$  in Fig. 1. Similarly, several IVD peaks between 11 and 16 MeV, which are obtained by including only IV interaction in RPA, are reorganized into, roughly speaking, one relatively broad peak with a center around 14 MeV, when IS interaction is further included in RPA. This is what we have called "iS-iV pigmy resonance" in the subsec. III. A. We have found that the structure of the pigmy resonance in  $^{24}\text{O}$  is very similar to that in  $^{22}\text{O}$ .

#### IV. SUMMARY AND DISCUSSIONS

The IV peak induced by IS correlation, the IS peak induced by IV correlation, and the possible collective states made by both IS and IV correlations in  $N \neq Z$  nuclei are studied by taking  $^{22}\text{O}$  and  $^{24}\text{O}$ . The spin-parity of the states is  $1^-$ , consequently, the excitation mode in the IV channel is IVD which has been well studied both experimentally and theoretically, while that in the IS channel is ISCD which has been theoretically pretty well studied though the related experimental information is still rather limited. Those light neutron-drip-line nuclei are chosen to study the present topic, mainly because the peaks with an appreciable amount of the strength of ISCD and those of IVD may be expected in the same energy region.

Taking the example of QGR in  $^{48}\text{Ca}$ , in Ref. [3] it is shown that a sharp appreciable IV peak appears at the energy of the IS QGR when both IS and IV interactions are taken into account while no peak of such IV strength is found if only IS interaction is included. This is one of the typical phenomena, in which IS collective modes in nuclei with  $N > Z$  may contain some IV strength.

As examples of the phenomena in which IV collective modes induce some IS strength in nuclei with  $N > Z$ , in the present work we have shown the peak at 18.5 MeV in  $^{22}\text{O}$  as well as the peak at 16.7 MeV in  $^{24}\text{O}$ .

Furthermore, in both  $^{22}\text{O}$  and  $^{24}\text{O}$  we have obtained the relatively-broad medium-size peak around 14 MeV, which is much lower than both ISCD GR and IVD GR and several MeV higher than the threshold energy. The peak contains both IS and IV correlations. We call the peak "iS-iV pigmy resonance". Indeed, the IV component of the pigmy resonance is clearly the result of reorganizing several IV peaks that are obtained by including only IV interaction in RPA. The reorganization could occur via the IS component contained in those several IV peaks.

In the present work together with the IS QGR example of  $^{48}\text{Ca}$  in Ref. [3] it is explicitly shown that in the scattering by IS (IV) particles some IV (IS) strength in addition to IS (IV) strength may be populated, in the case that target nuclei have  $N \neq Z$ . This can be understood as the result of the strong neutron-proton force, by which the isospin structure of normal modes is controlled. In a given nucleus with  $N \neq Z$  the ratio of the population of IV strength to that of IS strength by IS (or IV) particles seems to depend very much on the structure

of individual states.

As seen in Figs. 1 and 5, one may expect a large amount of ISCD strength in the energy region above the threshold energy and much lower than ISCD GR, when weakly-bound low- $\ell$  neutron levels are occupied in the ground state of nuclei and the particle state of the p-h components is a resonance (or almost resonance) in the continuum. If the particle state is bound, one may say that it is due to the so-called halo phenomenon in both particle and hole states. It may be very interesting to observe this phenomenon experimentally, though the actual strength of this kind of peak will depend rather sensitively on the actual one-particle energies of the particle and hole levels.

By using the material in the present paper, we have shown an important strong point of the method of solving the continuum RPA. Namely, when two (IS and IV) peaks occur in the continuum within respective widths, the transition densities of neutrons and protons for a given energy within the overlapped widths may not be uniquely determined, instead, they may depend on the (IS or IV) field operated externally. In contrast, if one uses the expansion of wave functions in terms of a finite number of basis wave-functions which have no intrinsic width, one can obtain only the transition densities of neutrons and protons which are determined uniquely for a given energy.

H. S. appreciates the partial support by JSPS KAKENHI Grant Numbers 16H02179.

- 
- [1] M. N. Harakeh and A. van der Woude, *Giant Resonances* (Clarendon Press, Oxford, 2001).
  - [2] A. Bohr and B. R. Mottelson, *Nuclear Structure* (Benjamin, Reading, MA, 1975), Vol.II.
  - [3] I. Hamamoto, H. Sagawa and X. Z. Zhang, *Phys. Rev. C* **55**, 2361 (1997).
  - [4] I. Hamamoto, H. Sagawa and X. Z. Zhang, *Phys. Rev. C* **57**, R1064 (1998).
  - [5] A. Leistenschneider, T.Aumann, K. Boretzky, D. Cortina, J. Cub, U. Datta Pramanik, W. Dostal, Th. W. Elze, H. Emling, H. Geissel *et al.*, *phys. Rev. Lett.* **86**, 5442 (2001).
  - [6] N. Nakatsuka, H.Baba, T.Aumann, R. Avigo, S. R. Banerjee, A. Bracco, C. Caesar, F.Camera, S. Ceruti, S. Chen *et al.*, *Phys. Lett. B* **768**, 387 (2017).
  - [7] E. Chabanat, P. Bonche, P.Haensel, J. Meyer, and F. Schaeffer, *Nucl. Phys.* **A635**, 231 (1998).

- [8] M. N. Harakeh and A. E. L. Dieperink, Phys. Rev. C **23**, 2329 (1981).
- [9] T. J. Deal, Nucl. Phys. **A217**, 210 (1973).

## Figures

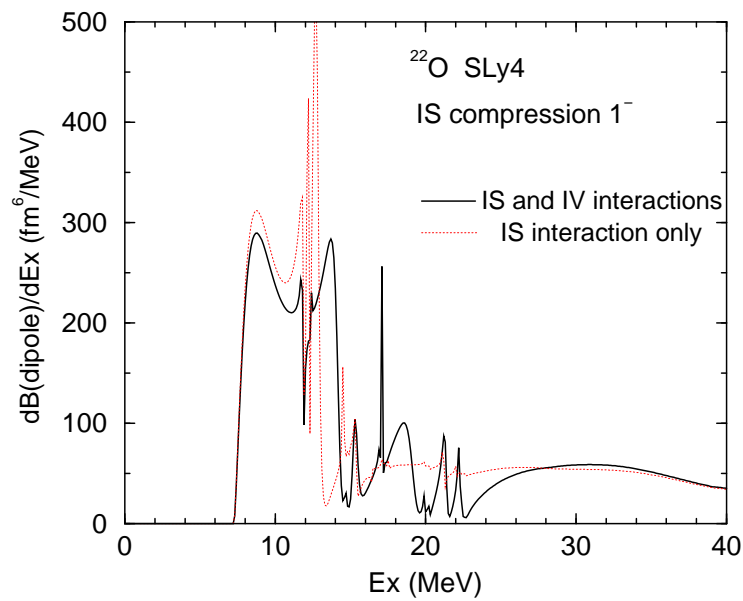


FIG. 1: (Color online) The RPA strength of isoscalar compression dipole (ISCD) of  $^{22}\text{O}$  calculated by using the SLy4 interaction as a function of excitation energy (Ex). The solid curve expresses the strength, in which both IS and IV interactions are included in RPA, while the dotted curve is obtained by including only IS interaction. No RPA solution is obtained below the threshold energy.

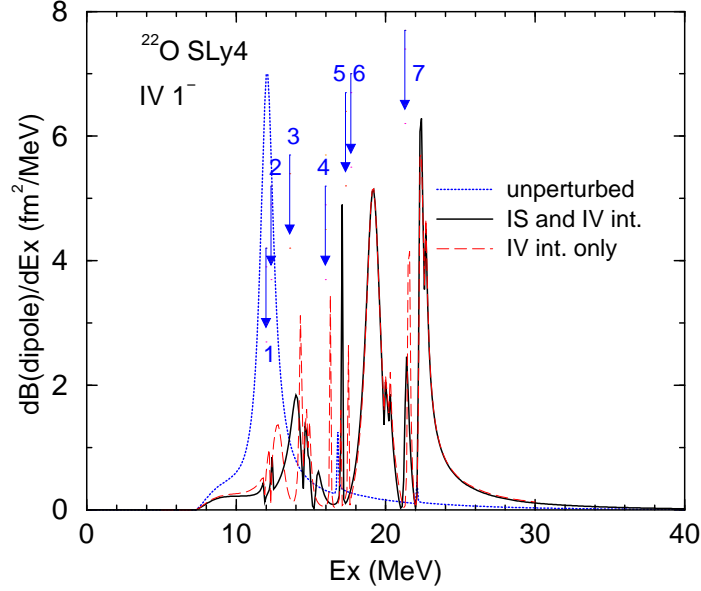


FIG. 2: (Color online) The RPA strength of isovector dipole (IVD) of  $^{22}\text{O}$  calculated by using the SLy4 interaction as a function of excitation energy. The solid curve expresses the strength obtained by including both IS and IV interactions in RPA, while the long-dashed curve is obtained by including only IV interaction in RPA. No RPA solution is obtained below the threshold energy. The unperturbed p-h strength, of which particle states are in the continuum, is denoted by the dotted curve, while the energies of the unperturbed p-h excitations, of which particle states are bound states, are denoted by vertical arrows. The numbered arrows correspond to the following (p-h) configurations: (1)  $(2s_{1/2}1p_{1/2}^{-1})_{\nu}$ , (2)  $(2s_{1/2}1p_{1/2}^{-1})_{\pi}$ , (3)  $(1d_{5/2}1p_{3/2}^{-1})_{\pi}$ , (4)  $(1d_{3/2}1p_{1/2}^{-1})_{\pi}$ , (5)  $(2s_{1/2}1p_{3/2}^{-1})_{\nu}$ , (6)  $(2s_{1/2}1p_{3/2}^{-1})_{\pi}$ , and (7)  $(1d_{3/2}1p_{3/2}^{-1})_{\pi}$ , respectively. The large unperturbed strength with a peak around 12 MeV denoted by the dotted curve is the neutron (p-h) =  $(1f_{7/2}1d_{5/2}^{-1})$  resonance.

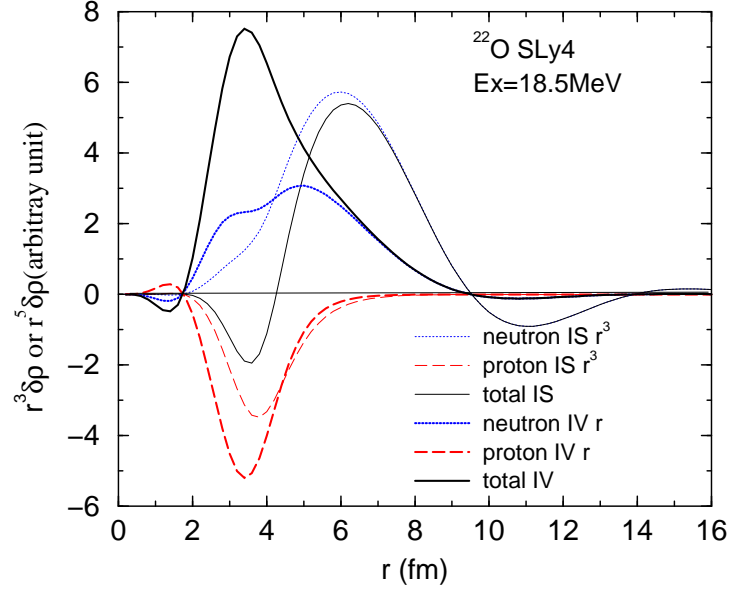


FIG. 3: (Color online) Radial transition densities multiplied by  $r^2 r^3$  for ISCD and those multiplied by  $r^2 r$  for IVD, which are calculated at  $E_x = 18.5$  MeV. Both IS and IV interactions are included. Note the relatively broad peak around 18.5 MeV denoted by the solid curve in Fig. 1 and the relatively broad peak with the center around 19 MeV expressed by the solid curve in Fig. 2. Thick curves are for ISCD, while thin curves are for IVD. Dotted curves are for neutrons, while long-dashed curves are for protons.



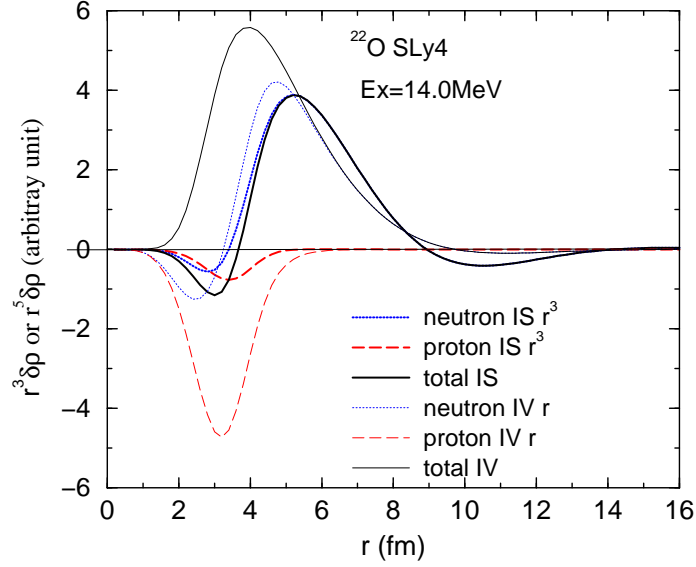


FIG. 4: (Color online) Radial transition densities multiplied by  $r^2 r^3$  for ISCD and those multiplied by  $r^2 r$  for IVD, which are calculated at  $E_x = 14.0$  MeV. Both IS and IV interactions are included. Note that the relatively broad peaks expressed by the solid curves appear around 14 MeV in both Figs. 1 and 2. Thick curves are for ISCD, while thin curves are for IVD. Dotted curves are for neutrons, while long-dashed curves are for protons.

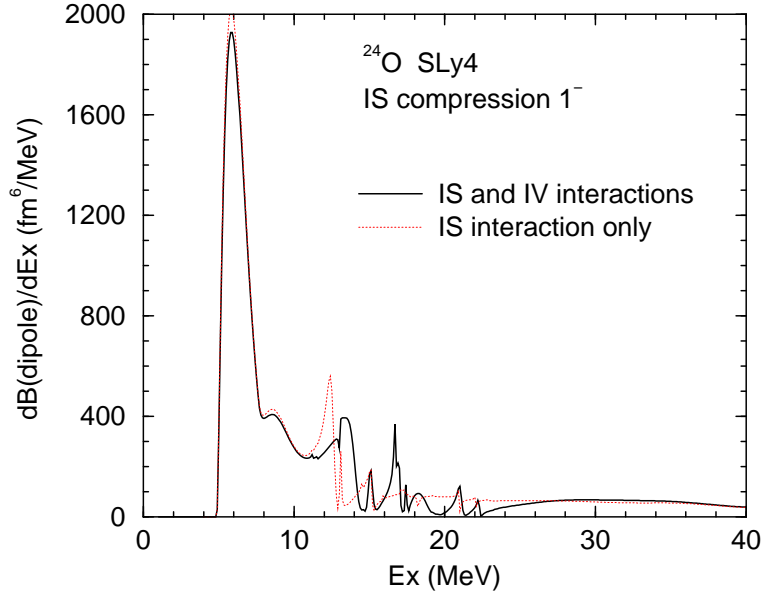


FIG. 5: (Color online) The RPA strength of isoscalar compression dipole of  $^{24}\text{O}$  calculated by using the SLy4 interaction as a function of excitation energy. The solid curve expresses the strength, in which both IS and IV interactions are included in RPA. The strength, in which only IS interaction is included in RPA, is denoted by the dotted curve. No RPA solution is obtained below the threshold energy.

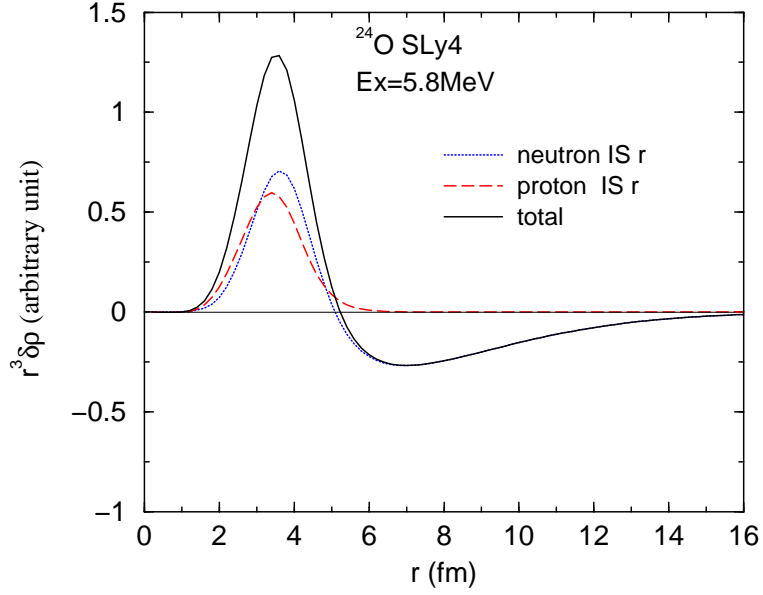


FIG. 6: (Color online)Radial transition densities that are multiplied by  $r^2r$  and expressed in arbitrary unit, which are calculated at  $E_x = 5.8$  MeV of  $^{24}\text{O}$  as a function of radial variable. Note that the peak energy of the huge response just above the threshold in Fig. 5 is 5.8 MeV. The neutron (proton) radial transition density is expressed by the dotted (long-dashed) curve, and the sum of the dotted and long-dashed curves is denoted by the solid curve.

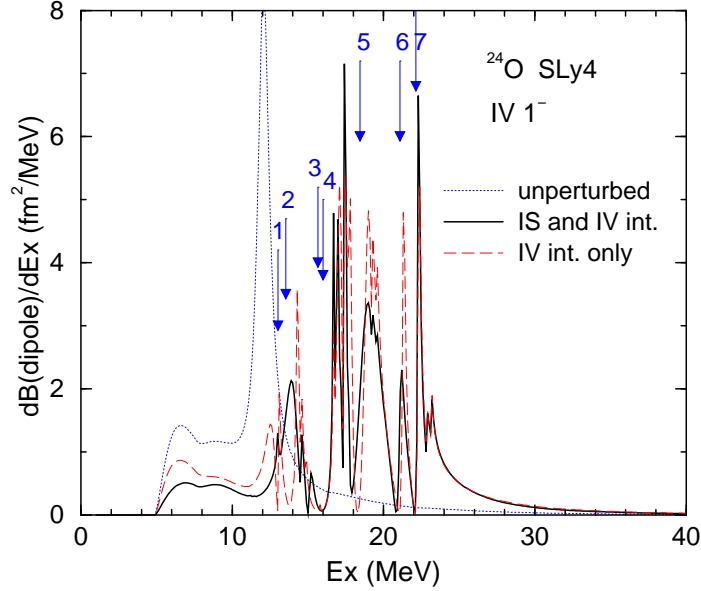


FIG. 7: (Color online) The RPA strength of isovector dipole of  $^{24}\text{O}$  calculated by using the SLy4 interaction as a function of excitation energy. The strength, in which both IS and IV interactions are included in RPA, is shown by the solid curve, while the strength, in which only IV interaction is included in RPA, is denoted by the long-dashed curve. No RPA solution is obtained below the threshold energy. The dotted curve expresses the unperturbed strength, in which particle states in p-h excitations are in the continuum. The energies of the unperturbed p-h excitations, of which particle states are bound, are denoted by vertical arrows. The numbered arrows correspond to the following (p-h) configurations: (1)  $(2s_{1/2}1p_{1/2}^{-1})_{\pi}$ , (2)  $(1d_{5/2}1p_{3/2}^{-1})_{\pi}$ , (3)  $(1d_{3/2}1p_{1/2}^{-1})_{\pi}$ , (4)  $(1d_{3/2}1p_{1/2}^{-1})_{\nu}$ , (5)  $(2s_{1/2}1p_{3/2}^{-1})_{\pi}$ , (6)  $(1d_{3/2}1p_{3/2}^{-1})_{\pi}$ , and (7)  $(1d_{3/2}1p_{3/2}^{-1})_{\nu}$ , respectively.